Spectroscopic properties of phenolic and quinoid carotenoids: a combined theoretical and experimental study

Christel M. Marian,*[a] Sebastian C. Kock,[b] Claas Hundsdörfer,[b] Hans-Dieter Martin,[b] Wilhelm Stahl,[c] Evgeny Ostroumov,[d] Marc G. Müller[d] and Alfred R. Holzwarth[d]

Received 26th August 2008, Accepted 31st October 2008
First published as an Advance Article on the web 15th December 2008
DOI: 10.1039/b814713b

For the natural carotenoid 3,3′-dihydroxyisorenieratene (DHIR) and two synthetic derivatives, 3,3′-dihydroxy-16,17,18,16′,17′,18′-hexanor-Φ,Φ-carotene (DHHC) and Φ,Φ-carotene-3,3′-dione (DHIRQ, isorenieratene-3,3′-dione), steady state absorption experiments and combined density functional and multi-reference configuration interaction calculations were carried out. In addition, femtosecond transient absorption spectra were recorded for DHIR. Due to their marked out-of-plane distortion in DHIR, the phenolic end groups participate only partially in the conjugation system. In the low-energy regime its absorption spectrum with the maximum at 21 700 cm^{-1} in acetone solution therefore closely resembles that of β-carotene, the same as for the T_1 energy. Further similarities are also found for the decay kinetics of the optically bright $1^1B_u^+$ state of these compounds. After femtosecond excitation, the $1^1B_u^+$ population of DHIR decays with a lifetime of 110 fs to the vibrationally hot $2^1A_g^-$,v state which in turn relaxes to the $2^1A_g^-$,0 state within 500 fs. Decay of the $2^1A_g^-$,0 state to the S_0 state occurs at a time scale of 12 ps. Demethylation of the phenolic end groups alleviates the steric repulsion by the polyene chain and causes a small red shift (1000 cm^{-1}) comparing the absorption spectra of DHHC and DHIR. Oxidation of DHIR leads to drastic changes of the electronic and geometric properties. The quinoid end groups of DHIRQ are fully integrated into the conjugation system, shifting the absorption maximum to 17 800 cm^{-1} in acetone solution which thus takes a blue color. The results of the quantum chemical calculations indicate that, in addition to the $2^1A_g^-$ (S_1) state, two dark internal charge-transfer singlet states and the $1^1B_u^-$ state might be located energetically below the optically bright $1^1B_u^+$ (S_5) state of DHIRQ.

Introduction

More than 600 different natural carotenoids have been isolated until now but only a few of them carry an aromatic substructure. 3,3′-Dihydroxyisorenieratene (DHIR) is an unusal phenolic carotenoid present in the membrane of *Brevibacterium linens* which is used in the dairy industry for the bacterial fermentation of various red smear cheeses.[1,2] According to its structural properties DHIR acts as a bifunctional antioxidant and photoprotecting agent against lipid, protein and DNA damage.[3,4] Free radical scavenging effects and inhibition of UV-induced lipid oxidation are likely related to the redox activity of both phenolic groups and the core system of conjugated double bonds. The corresponding quinone, *Φ*,*Φ*-carotene-3,3′-dione (DHIRQ, isorenieratene-3,3′-dione), is found as the resulting two-electron oxidation product. Alternating double bonds also provide the structural prerequisite for DHIR being an efficient singlet oxygen quencher. UV absorption due to the presence of the aromatic rings is likely responsible for the protection of DNA against UVB-induced thymidine dimer formation by DHIR as shown in human fibroblasts.[3]

In contrast to other carotenoids, little is known about the electronic states of their aromatic congeners. It is likely, however, that aromatic substitutents affect the geometry of the molecule and thus influence the energy levels. In addition to DHIR, another phenolic carotenoid, 3,3′-dihydroxy-16,17,18,16′,17′,18′-hexanor-*Φ*,*Φ*-carotene (DHHC), was studied which lacks the methyl groups attached to the phenyl rings and thus minimizes the steric hindrance between the end groups and the polyene chain.

It is firmly established that the single excitation from the highest occupied molecular orbital (HOMO) to the lowest unoccupied molecular orbital (LUMO) ($1^1B_u^+$) does not constitute the S_1 state of linear polyenes and related compounds.[5,6] Instead, the wave function of the lowest excited singlet state ($2^1A_g^-$) is a linear combination of many configurations with large coefficients, with the leading term being doubly excited with respect to the electronic ground state ($1^1A_g^-$).[7] The radiative transition between the S_1 state and the electronic ground state is dipole forbidden but becomes weakly allowed by vibronic coupling to the optically bright $1^1B_u^+ \rightarrow 1^1A_g^-$ transition. In shorter polyenes

[a]*Institute of Theoretical and Computational Chemistry, Heinrich-Heine-University Düsseldorf, Universitätsstr. 1, 40225, Düsseldorf, Germany. E-mail: Christel.Marian@uni-duesseldorf.de; Fax: +49 211 8113466; Tel: +49 211 8113210*
[b]*Institute of Organic and Macromolecular Chemistry, Heinrich-Heine-University Düsseldorf, Universitätsstr. 1, 40225, Düsseldorf, Germany. E-mail: martin@uni-duesseldorf.de; Fax: +49 211 8114324; Tel: +49 211 8112298*
[c]*Institute of Biochemistry and Molecular Biology I, Heinrich-Heine-University Düsseldorf, Universitätsstr. 1, 40225, Düsseldorf, Germany. E-mail: wilhelm.stahl@uni-duesseldorf.de; Fax: +49 211 8113029; Tel: +49 211 8112711*
[d]*Max-Planck-Institut für Bioanorganische Chemie, Stiftstr. 34-36, 45470, Mülheim a.d. Ruhr, Germany. E-mail: holzwarth@mpi-muelheim.mpg.de; Fax: +49 208 3063951; Tel: +49 208 3063571*

where Kasha's rule is well fulfilled fluorescence originates mainly from the $2^1A_g^- \rightarrow 1^1A_g^-$ emission whereas in polyenes with larger conjugation lengths (N ≥ 6) primarily $1^1B_u^+ \rightarrow 1^1A_g^-$ emission is observed.[8] The question whether the $1^1B_u^+$ state actually represents the S_2 state or is rather the S_3 state has been a matter of controversial debates in recent years: An intermediate state which turns up in resonance Raman and time-resolved femtosecond excitation spectra of natural carotenoids is interpreted either as a further low-lying electronic state ($1^1B_u^-$)[9–16] or an excited vibronic level of the S_1 state.[17,18] Recent theoretical investigations on the conjugation length dependence of the low-lying states of linear polyenes, α,ω-diphenylpolyenes, and (mini-)β-carotenes (short-chain analogues) indicate that the $1^1B_u^-$ state might indeed be the S_2 state in chromophores with long polyene chains.[19,20] According to these studies, the crossover point is strongly geometry dependent though, thus intersections between the $1^1B_u^-$ and $1^1B_u^+$ potential energy surfaces are to be expected for carotenes with conjugation lengths N > 9. This model could also explain the experimentally observed conjugation length dependence of relaxation kinetics in β-carotene homologues.[21] It will be interesting to see whether such curve crossings can be found for the three carotenoids investigated here.

Carbonyl groups are known to change the spectroscopic properties of carotenoids markedly.[22] There is theoretical and spectroscopic evidence that carbonyl carotenoids possess a low-lying internal charge-transfer (ICT) state that participates in the relaxation process after photoexcitation.[23,24] In the naturally occurring carotenoids peridinin and fucoxanthin which are present in the light-harvesting antennae of algae, the carbonyl group is attached to the polyene chain whereas it is part of the quinonoid system in DHIRQ. The question therefore arises whether ICT states are found among the low-lying electronic states of DHIRQ, too.

It is customary to employ the approximate symmetry labels of planar polyenes (C_{2h} molecular point group) for the designation of the electronic states of carotenoids. In addition, the state labels carry + and − superscripts which denote the pseudoparity character of a state introduced by Pariser.[25] In this model, only transitions $A_g^+ \leftrightarrow B_u^-$ and $A_g^- \leftrightarrow B_u^+$ are allowed. These pseudoparity rules are not strictly obeyed, however: due to configuration interaction $A_g^- \leftrightarrow B_u^-$ transitions can also yield some intensity. Wherever possible, we will use the Pariser nomenclature and revert to the strict symmetry classification only when necessary. A_u and B_g states do not play a role in the low-energy regime of polyenes. As we will see later, however, the low-lying ICT states of DHIRQ belong to these irreducible representations.

Experimental procedures and computational details

Experimental

3,3′-Dihydroxyisorenieratene (DHIR), 3,3′-dihydroxy-16,17,18,16′,17′,18′-hexanor-*Φ*,*Φ*-carotene (DHHC) and *Φ*,*Φ*-carotene-3,3′-dione (DHIRQ, isorenieratene-3,3′-dione) (Scheme 1) were synthesized according to a prescription published elsewhere.[3,4] The absorption spectra were measured on a Perkin-Elmer Lambda 19 spectrometer. The wavelength of the $1B_u^+ \leftrightarrow 1A_g^-$ transition of polyenes is known to be strongly dependent on the polarizability of the solvent.[26] Thus, the spectra of all three carotenoids should be measured in the same solvent. However, due to striking differences in the solubility, we pursued the strategy of finding solvents of similar polarity and polarizability in which at least two of the three substances are soluble to an extent sufficient for recording absorption spectra. The absorption spectra of DHIR and DHHC were recorded in tetrahydrofuran (THF), those of DHIR and DHIRQ in acetone. Analytical grade (Uvasol) THF and acetone were used as purchased from Merck. However, for the relatively high concentrations (corresponding to OD = 8 per cm at the absorption maximum), required for the femtosecond transient absorption measurements, ethanol was preferred as the solvent in order to avoid any aggregation.

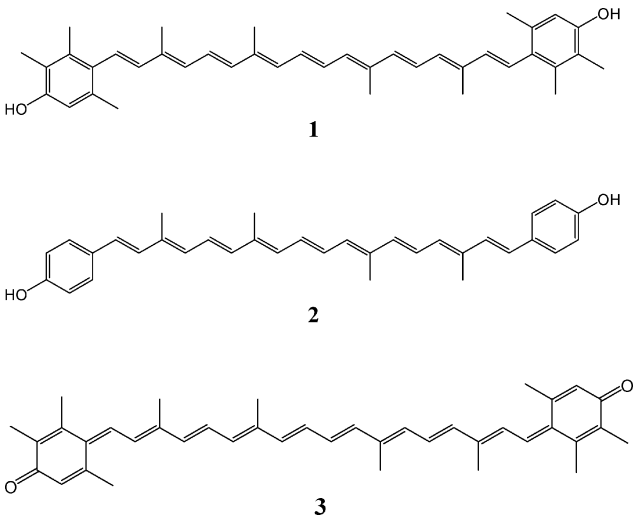

Scheme 1 **1** 3,3′-dihydroxyisorenieratene (DHIR), **2** 3,3′-dihydroxy-16,17,18,16′,17′,18′-hexanor-*Φ*,*Φ*-carotene (DHHC), **3** *Φ*,*Φ*-carotene-3,3′-dione (DHIRQ, isorenieratene-3,3′-dione).

Femtosecond transient absorption measurements of DHIR were performed as described earlier.[27] The excitation pulse width was ~80–90 fs, FWHM of ~4 nm, with an intensity of ~1.9×10^{14} photons per cm^2 per pulse. All measurements were performed in a 1 mm cuvette which was moved in a Lissajous scanner during exeriments in order to avoid over-excitation and destruction of the sample. Sample stability was controlled by the absorption spectrum which was essentially the same before and after the measurements.

Data were analyzed as lifetime distributions and are shown as lifetime density maps,[27] which are calculated by an inverse Laplace transformation from the original transient absorption surfaces *vs.* time and represent the amplitudes of the lifetime components in a quasi-continuous lifetime range. White-yellow regions correspond to positive amplitudes and reflect either absorption decay or rise of a bleaching. Blue-black regions correspond to negative amplitudes and reflect either absorption rise or decay of the bleaching.

Calculations

Throughout this work a split valence basis set with d polarization function on all non-hydrogen atoms (SV(P)) was used.[28] Tests on smaller α,ω-diphenylpolyenes had shown that the electronic excitation energies obtained in this basis are practically converged with respect to the basis set quality.[19] The geometries of the

electronic ground states were determined by Kohn–Sham (KS) density functional theory (DFT) using the B3LYP hybrid functional.[29–31]

The electronic structures of the optically bright $1^1B_u^+$ excited state and the first excited triplet state T_1 ($1^3B_u^+$) are governed by single excitations. Time dependent density functional theory (TDDFT)[32] can therefore be employed for the $1^1B_u^+$ excited state geometry optimization while unrestricted density functional theory (UDFT) is favorably applied for the corresponding triplet. The other two low-lying singlet states of carotenoids, $2^1A_g^-$ and $1^1B_u^-$ exhibit strong multi-configuration character, with the leading configuration being doubly excited with respect to the electronic ground state. Single-reference linear response methods, such as TDDFT, are therefore not appropriate. We have refrained here from searching for the minimum nuclear structures of these states and report only single-point energies. All geometry optimizations were performed with the Turbomole 5.7 package.[33] Solvent effects were not included in the calculations.

A parallelized version of the combined density functional theory/multireference configuration interaction (DFT/MRCI) method[20,34] was used for single-point energy calculations at the (TD)DFT equilibrium geometries. The configuration state functions (CSFs) in the MRCI expansion are built up from KS orbitals using the BH-LYP[31,35] functional. A common set of reference CSFs was used for all spatial symmetries. The 1s shells of the carbon atoms were kept frozen in the electron correlation treatment. The initial MRCI reference space was spanned by all single and double excitations from the five highest occupied molecular orbitals (MOs) to the five lowest unoccupied MOs of the ground state KS determinant. In these preliminary calculations an orbital selection threshold of 0.6 E_h was employed and for DHIR and DHHC the six lowest roots in A_g and A_u/B_u symmetries were determined. The final reference space consisted of all configurations which contributed with a squared coefficient of at least 0.003 to one of the roots in the first DFT/MRCI runs. Wave functions and excitation energies were computed for five ^1A_g and four $^1A_u/^1B_u$ states as well as four ^3A_g and four $^3A_u/^3B_u$ states in the final DFT/MRCI runs using the tighter selection threshold of 1.0 E_h originally recommended by Grimme and Waletzke.[34] For the quinone which exhibits C_{2h} symmetry, DFT/MRCI calculations on more states were carried out, *i.e.*, we solved the CI secular equation for six ^1A_g, two ^1A_u, two ^1B_g, and five ^1B_u states as well as five ^3A_g, two ^3A_u, two ^3B_g, and six ^3B_u states.

Results and discussion

Ground state geometry

The DHIR and DHHC ground state potential energy minima turned out to correspond to twisted nuclear structures. This means that their electronic wave functions transform according to the irreducible representations A_g and A_u of the C_i molecular point group, *i.e.*, only inversion symmetry is preserved. In the electronic ground state, the polyene chains exhibit a pattern of alternating single and double bonds. The central bond of the phenolic carotenoids has double bond character. Due to steric hindrance between the methyl groups in *ortho* position of the phenyl rings and hydrogen atoms of the polyene chain, the equilibrium geometry of DHIR corresponds to a structure where the phenyl rings are markedly twisted out of plane (torsion angle ≈ 37°). The planar nuclear arrangement of the rings represents a saddle point on the potential energy surface located roughly 2100 cm^{-1} (25 kJ mol^{-1}) above the minimum. DHHC which lacks these methyl groups was expected to have a planar equilibrium structure, but this is actually not the case. The molecule is S-shaped with the phenyl groups twisted out of the plane of the polyene backbone by about 8°. Constraint optimization in C_{2h} symmetry yields a saddle point about 1000 cm^{-1} (12 kJ mol^{-1}) above the minimum. In the quinone DHIRQ, however, the stabilization due to conjugation is larger than the steric repulsion. As a consequence, a planar minimum structure is found here. In this molecule, the pattern of single and double bonds in the polyene chain is shifted by one unit as expected for a quinoid structure.

Characterization of the electronic states and steady-state absorption

Computed vertical excitation energies of all compounds at their respective ground state geometries are collected in Table 1. For the optically bright $1^1B_u^+$ state these data are compared with experimental absorption maxima. According to the calculations, the first excited singlet state is the $2^1A_g^-$ state in all compounds studied here. It exhibits pronounced multi-configuration character: in addition to the leading ($\pi_{HOMO}^2 \rightarrow \pi_{LUMO}^2$) configuration and other double excitations such as ($\pi_{HOMO-1}\pi_{HOMO} \rightarrow \pi_{LUMO}\pi_{LUMO+1}$) large contributions from single excitations of the type ($\pi_{HOMO-1} \rightarrow \pi_{LUMO}$) and ($\pi_{HOMO} \rightarrow \pi_{LUMO+1}$) are found in the MRCI expansion. Absorption is not observable for the $2^1A_g^-$ state because the electric

Table 1 Calculated singlet vertical excitation energies T_v [cm^{-1}] in comparison with experimental absorption band maxima [cm^{-1}]. Oscillator strengths f(r) of allowed one-photon transitions are given in parentheses

	1^3B_u	$2^1A_g^-$	$1^1A_u/1^1B_g$	$1^1B_u^-$	$1^1B_u^+$		$3^1A_g^-$
Compound	T_v	T_v	T_v	T_v	T_v	Exp.	T_v
DHIR min.	8600	15 900		21 000 (0.19)	18 400 (4.05)	21 500[a], 21 700[b]	24 700
DHIR planar[c]	7000	12 900		18 200 (0.42)	16 600 (3.96)		22 600
DHHC min.	8300	15 100		19 900 (0.19)	17 900 (4.11)	20 700[a]	24 400
DHHC planar[d]	7000	12 900		18 200 (0.39)	16 900 (3.85)		22 800
DHIRQ	6700	10 100	14 400/14 400	14 800 (0.63)	15 600 (4.30)	17 800[b]	17 200
β-Carotene	8800[e]	16 000[e]		21 400 [e](0.31)	19 500 [e](3.66)	21 800[f]	25 800[e]

[a] This work, in tetrahydrofuran solution. [b] This work, in acetone solution. [c] Saddle point (2100 cm^{-1} above min.). [d] Saddle point (1000 cm^{-1} above min.). [e] Ref. 20, DFT/MRCI results. [f] Ref. 43 in *n*-hexane solution.

dipole transition from the electronic ground state is one-photon-forbidden. The optically bright $1^1B_u^+$ state is mainly characterized by a ($\pi_{HOMO} \rightarrow \pi_{LUMO}$) single excitation from the electronic ground state. For the two hydroquinones it constitutes the second excited singlet state in the vertical excitation spectrum while it yields the fifth excited singlet state in DHIRQ, with the $2^1A_g^-$ and $1^1B_u^-$ states and a pair of optically dark ^1A_u and ^1B_g states lying below $1^1B_u^+$ (see discussion below). Isosurfaces of the orbital amplitudes of the π_{HOMO-1}, π_{HOMO}, π_{LUMO}, and π_{LUMO+1} orbitals of DHIRQ are shown in Fig. 1. Due to the increased conjugation length of this compound, the $1^1B_u^-$ state, which has large coefficients for the double excitations ($\pi_{HOMO}^2 \rightarrow \pi_{LUMO}\pi_{LUMO+1}$) and ($\pi_{HOMO-1}\pi_{HOMO} \rightarrow \pi_{LUMO}^2$), is energetically stabilized and is thus favored over the $1^1B_u^+$ state. The presence of an electronic state intermediate between S_1 and S_2 was predicted for polyenes with conjugation length $N \geq 9$ and β-carotenes with $N \geq 11$.[19,20] It is believed to play an important role in the relaxation processes following the primary photo-excitation.[22] The configuration with the largest coefficient in the DFT/MRCI expansion of the $^1B_u^-$ state ($\pi_{HOMO-2} \rightarrow \pi_{LUMO}$) is singly excited with respect to the $1^1A_g^-$ ground state. Since the $1^1B_u^+$ and $1^1B_u^-$ states belong to the same irreducible representation A_u (B_u) of the true C_i (C_{2h}) molecular point group of the carotenoids, also the ($\pi_{HOMO} \rightarrow \pi_{LUMO}$) configuration is allowed to mix into the $^1B_u^-$ wave function. A small contribution of the ($\pi_{HOMO} \rightarrow \pi_{LUMO}$)

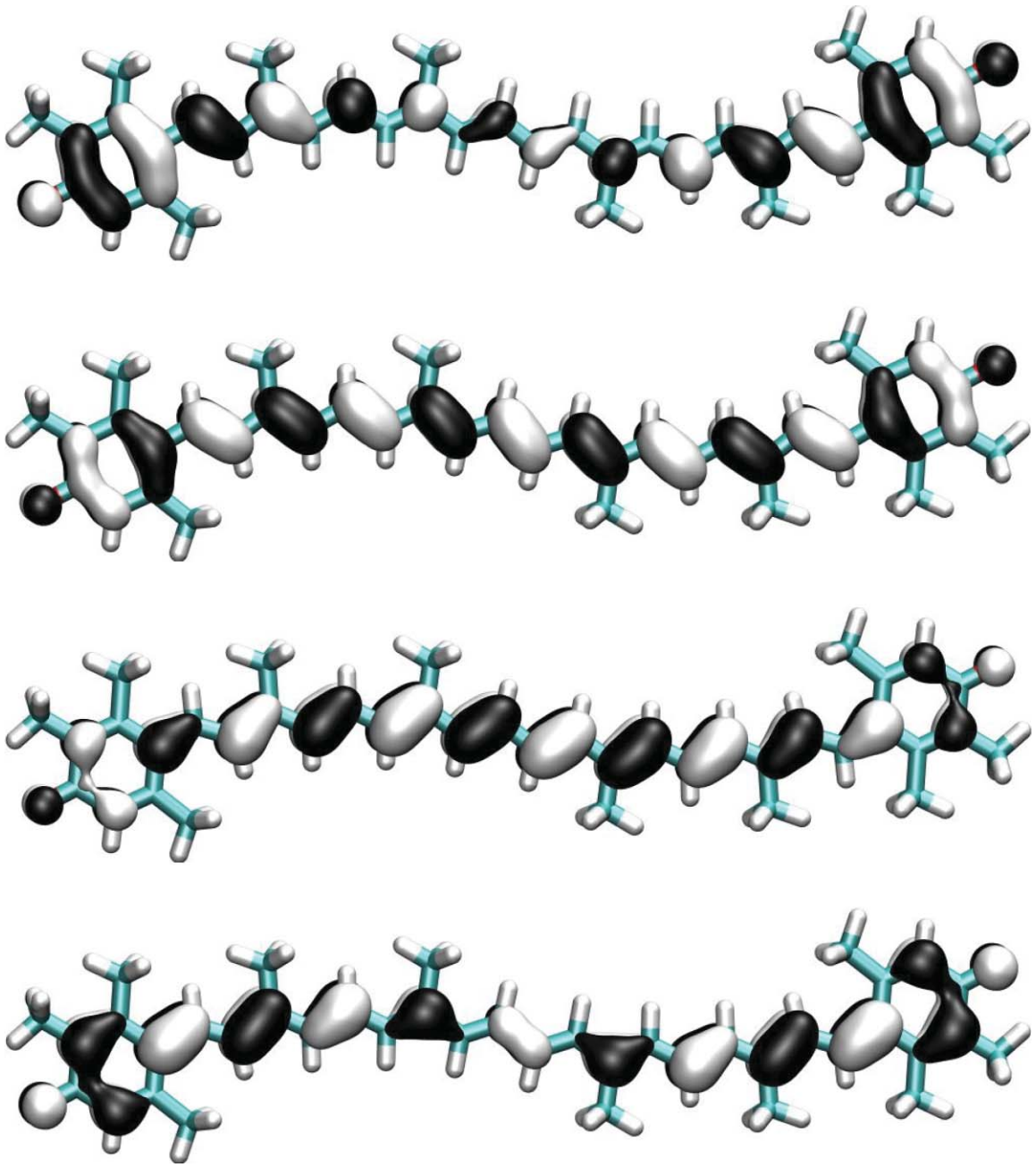

Fig. 1 Orbital amplitudes (isosurface 0.03) of frontier orbital of DHIRQ. Orbitals are displayed in energetic order. From bottom to top: $13a_u = \pi_{HOMO-1}$, $13b_g = \pi_{HOMO}$, $14a_u = \pi_{LUMO}$, $14b_g = \pi_{LUMO+1}$.

configuration is sufficient to lend some oscillator strength to the $1^1B_u^- \leftrightarrow 1^1A_g^-$ transition (see Table 1). Due to the energetic proximity of the $1^1B_u^+$ and $1^1B_u^-$ states—or even reversal of their energetic order—upon geometry relaxation on the excited state potential energy surface (see next section), this transition will probably be buried under the bright $1^1B_u^+ \leftrightarrow 1^1A_g^-$ band. The $3^1A_g^-$ state, which has also been discussed intensively in the literature[7,22,36] is located clearly above the $1^1B_u^+$ state in our calculations. Its electronic structure is dominated by single excitations ($\pi_{HOMO-1} \rightarrow \pi_{LUMO}$), ($\pi_{HOMO-3} \rightarrow \pi_{LUMO}$), and ($\pi_{HOMO} \rightarrow \pi_{LUMO+1}$) and the doubly excited ($\pi_{HOMO-2}\pi_{HOMO} \rightarrow \pi_{LUMO}^2$) configuration which exhibits two open shells, too. Configurations with four open shells that might correspond to a combination of two triplet states as proposed by Tavan and Schulten[7] play only an underpart in the DFT/MRCI wave function expansion.

Absorption spectra, recorded in THF, acetone, and ethanol solutions at room temperature, are shown in Fig. 2 and 3. The spectra of DHHC and DHIRQ could not be measured in the same solvent due to striking differences in solubility. DHIR is soluble in all applied solvents. The maxima of the DHIR absorption bands in THF (466 nm), acetone (460 nm) or ethanol (458 nm) appear at about equal wavelengths proving that the solvatochromic shifts brought about by these solvents are comparable. Because of the marked out-of-plane distortion of the phenyl groups, DHIR exhibits an effective conjugation length comparable to that of β-carotene which carries β-ionylidene rings as end groups. The band maximum of the DHHC absorption (483 nm in THF) is clearly red shifted with respect to the DHIR value, indicating that the phenyl

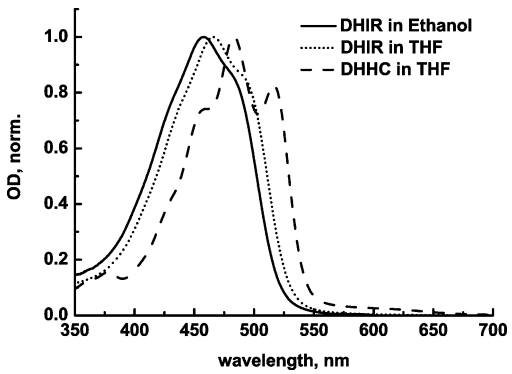

Fig. 2 Absorption spectra of DHIR in ethanol (solid line) and THF (dotted line), and DHHC in THF (dashed line).

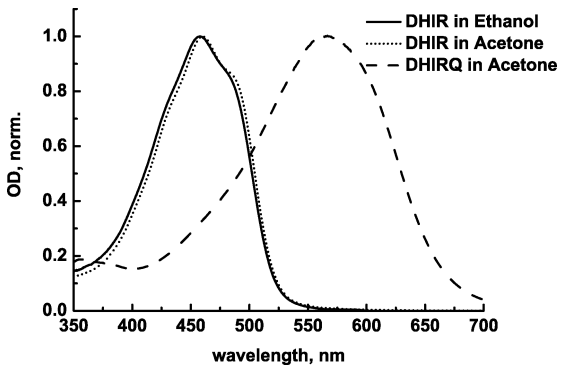

Fig. 3 Absorption spectra of DHIR in ethanol (solid line) and acetone (dotted line), and DHIRQ in acetone (dashed line).

rings are partially integrated in the conjugated π system of DHHC. The DHHC band exhibits pronounced vibrational structure so that the 0–0 peak at 517 nm (19 340 cm^{-1}) can be easily identified, in contrast to DHIR where the origin transition appears only as a shoulder in the spectrum. Oxidation of DHIR to the planar quinone form leads to complete loss of vibrational structure and a strong red shift of the absorption maximum (563 nm in acetone). Solutions of DHIRQ in acetone thus take a blue color. Lack of vibrational structure is quite typical for ICT states.

Direct comparison of the absorption maxima with the theoretical vertical $1^1B_u^+ \leftarrow 1^1A_g^-$ transition energies (Table 1) shows that the results obtained with the DFT/MRCI method consistently underestimate the wave numbers of the experimental band maxima by about 2000–3000 cm^{-1}, but the general trends are correct. Moreover, from the results of the benchmark calculations[19,20] on linear polyenes, α,ω-diphenylpolyenes, and (mini-)β-carotenes it can be expected that the energy gap between the $1^1B_u^+$ and $2^1A_g^-$ states is well reproduced by the DFT/MRCI method. At present this method appears to be the only one suitable to predict the correct order of electronic states in long polyenes and carotenoids; high-level *ab initio* methods such as CASPT2 or CC3 are too time-consuming.[37] Calculated vertical excitation energies of planar constraint DHIR and DHHC are practically indistinguishable showing only a minor electronic effect of the methyl substituents in *ortho* and *meta* positions. The spectral shift is therefore mainly ascribed to the steric effect of the methyl groups in *ortho* position on the torsion angle of the phenyl rings.

DHIRQ is exceptional among the three compounds studied here in that it has a planar equilibrium geometry and possesses two C=O groups which are part of the conjugated π system. At the C=O groups two high-lying doubly occupied orbitals are located which are best characterized as n orbitals (Fig. 4). Excitation of an electron from these in-plane orbitals to π_{LUMO} and π_{LUMO+1} (Fig. 1) yields a pair of optically dark ^1A_u and ^1B_g states (as well as corresponding triplets) which are near-degenerate with $1^1B_u^+$ and $1^1B_u^-$ (see Table 1). Since π_{LUMO} is delocalized over the whole polyene chain, the low-lying $^{1,3}A_u$ and $^{1,3}B_g$ states exhibit partial internal charge-transfer character. Due to the high symmetry of the isolated molecule, one radical site is delocalized over both oxygen atoms. However, the two states are degenerate (within the accuracy of the calculations). A small perturbation will therefore suffice to localize the unpaired electron at one of the oxygen atoms.

Furthermore, it is noteworthy that the energy gap between the optically bright $1^1B_u^+$ state and the S_1 ($2^1A_g^-$) state significantly increases when DHIR is oxidized to DHIRQ, a direct consequence of the increased conjugation length which favors doubly excited configurations.

Relaxed excited states and transient absorption spectra

The triplet energy levels of DHIR, DHHC, or DHIRQ were not determined experimentally. In order to judge the reliability of the theoretical predictions, we compare relaxed energies, computed for β-carotene with the same quantum chemical approach,[20] with literature values. A thermochemical value of 81.1 ± 4.2 kJ mol^{-1} (≈6800 cm^{-1}) was reported for the relaxed energy level of the first excited triplet (T_1) state of β-carotene dissolved in benzene.[38] A somewhat higher value of 88 ± 3 kJ mol^{-1} (≈7400 cm^{-1})

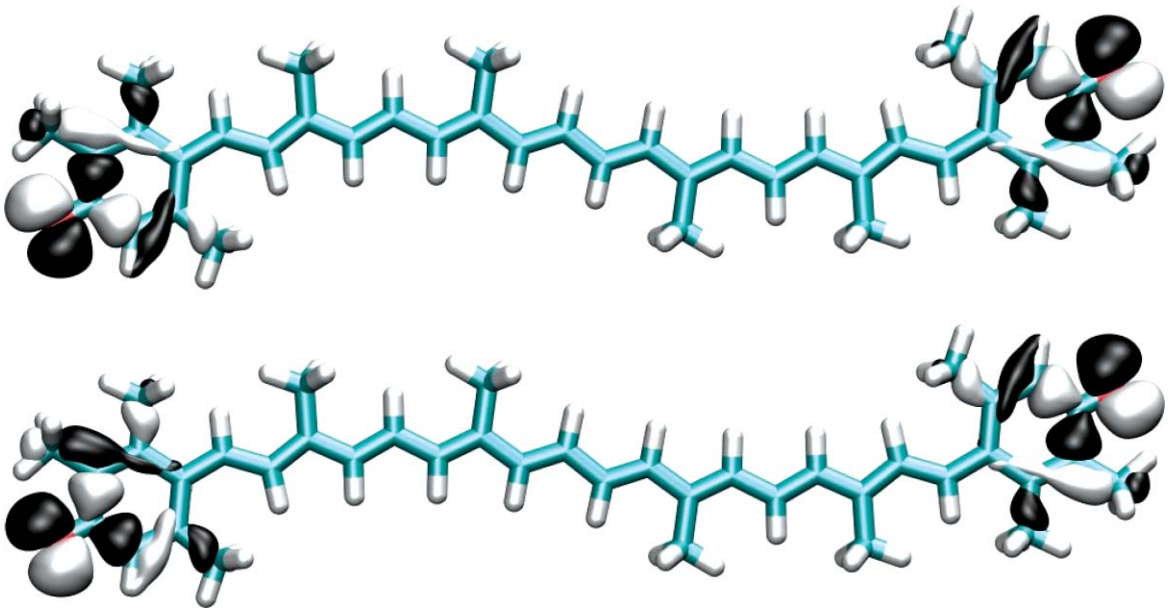

Fig. 4 Orbital amplitudes (isosurface 0.03) of the highest occupied in-plane orbitals of DHIRQ: $62b_u$ (bottom), $63a_g$ (top).

was determined directly from phosphorescence in deuterated benzene.[39] The good agreement with our computed adiabatic energy is probably somewhat fortuitous: on the one hand, it has been shown that the DFT/MRCI method systematically underestimates the true gas phase excitation energies in polyenes and related compounds.[19,37] On the other hand, a bathochromic solvent shift of the T_1 level in polarizable solvents is expected, in analogy with the trends for the corresponding singlet state ($1^1B_u^+$). The first excited triplet of DHIR is seen to have approximately the same energy as the one of β-carotene whereas the planar DHIRQ exhibits a significantly lower T_1 energy. The barrier to planarity is very small on the T_1 potential energy surface of DHHC. The twisted T_1 minimum structure (dihedral angle 6°) and the planar saddle point have nearly identical energies.

The ability of a carotenoid to quench singlet oxygen requires a spectral overlap of its $T_1 \leftrightarrow S_0$ excitation with the $a^1\Delta_g \leftrightarrow X^3\Sigma_g^-$ transition of molecular oxygen. For the latter an adiabatic excitation energy of 7918 cm^{-1} was reported.[40–42] From an energetic point of view, DHIR, DHHC, and DHIRQ are therefore expected to be efficient singlet oxygen quenchers, in agreement with experimental observations.[3,4]

Proceeding to the $1^1B_u^+$ state, it is seen from a comparison of the entries in Tables 1 and 2 that the energy release on this potential energy surface upon geometry relaxation is rather small (between 1000 cm^{-1} for planar DHHC to 2000 cm^{-1} for DHIR). The relaxation energy of DHIR is larger because bond length alternation in the polyene chain is less pronounced in the excited state. This reduces the steric hindrance of the methyl groups in the *ortho* positions of the phenyl groups of DHIR resulting in a smaller out-of-plane distortion angle (28°) in comparison to the electronic ground state (37°). DHHC differs from DHIR in so far as the barrier to planarity is smaller than in the latter. The out-of-plane distortion of the phenol rings in the $1^1B_u^+$ excited state is roughly the same as in the ground state, but the barrier to planarity disappears almost completely on the excited potential energy hypersurface (≈100 cm^{-1}).

The geometry dependence of the doubly excited configurations is significantly larger than for the singly excited $1^1B_u^+$ state. Relaxation of the nuclear geometry in the latter state preferentially stabilizes the $2^1A_g^-$ and $1^1B_u^-$ states. While the energy gap between the $2^1A_g^-$ and $1^1B_u^+$ states increases when the excited state geometry is relaxed, the energy separation between the $1^1B_u^+$

Table 2 Calculated adiabatic excitation energies T_e of the $1^3B_u^+$ and $1^1B_u^+$ states. Vertical excitation energies T_v of the $2^1A_g^-$ and $1^1B_u^-$ states and the oscillator strengths f(r) of the $1^1B_u^+ \rightarrow 1^1A_g^-$ and $1^1B_u^- \rightarrow 1^1A_g^-$ transitions refer to the $1^1B_u^+$ minimum geometry

	$1^3B_u^+$	$1^1B_u^+$		$2^1A_g^-$	$1^1B_u^-$	
Compound	T_e/cm^{-1}	T_e/cm^{-1}	f(r)	T_v/cm^{-1}	T_v/cm^{-1}	f(r)
DHIR	6000	16 400	2.51	11 800	17 400	1.81
DHIR planar	4600	15 700	3.53	9600	14 700	0.71
DHHC	5600	16 800	2.88	11 100	16 000	1.41
DHHC planar	4600	15 900	3.63	9600	14 700	0.46
DHIRQ	4400	14 200	4.93	6800	12 000	0.00
β-Carotene[a]	6200	18 300	3.15	11 900	17 100	0.83

[a] Ref. 20, DFT/MRCI results.

and $1^1B_u^-$ states shrinks (DHIR) or undergoes a zero crossing (DHHC). This should have interesting consequences on the photophysics of these compounds. The mixed character of the $1^1B_u^+$ and $1^1B_u^-$ wave functions is reflected in the large oscillator strengths of the $1^1B_u^- \leftrightarrow 1^1A_g^-$ and the decreased values for the $1^1B_u^+ \leftrightarrow 1^1A_g^-$ transitions. In the planar constraint form of DHIR, the $1^1B_u^-$ state has dropped below the $1^1B_u^+$ state. The absolute $1^1B_u^-$ energy at this saddle point of the $1^1B_u^+$ potential energy surface is only marginally higher than the adiabatic $1^1B_u^+$ energy and it is expected to decrease further until the $1^1B_u^-$ minimum geometry is reached. Due to their energetic proximity strong vibronic coupling between the two states is expected.

Fig. 5 shows the original three-dimensional transient absorption data (Δ absorbance *vs.* wavelength *vs.* time-delay) for DHIR in ethanol excited at 493 nm for different time resolutions and wavelength ranges. The lifetime density map of these data (for all the data sets have been combined) is shown in Fig. 6 for the 500–710 nm spectral region. In the visible range two positive (500 fs and 12 ps) and one negative (110 fs) amplitude bands are observed. The 110 fs component is well known for carotenoids and represents the decay time of the initially excited $1^1B_u^+$ state, relaxing to the vibrationally hot $2^1A_g^-$,v state. The kinetic scheme is shown in Fig. 7. The following vibrational relaxation occurs with a lifetime of 500 fs to the vibrationally relaxed $2^1A_g^-$,0 state. The difference spectrum of the $2^1A_g^-$ is also well known for non-aromatic carotenoids and has a strong excited state absorption (ESA) band in the 550–600 nm region (12 ps component, Fig. 6). According to preliminary calculations involving ten roots in ^1A_u symmetry, this strong ESA band corresponds mainly to a ($\pi_{LUMO} \rightarrow \pi_{LUMO+1}$) excitation. The lifetime of 12 ps represents the relaxation of the $2A_g^-$,0 state to the ground state. Overall the decay scheme is very similar to that of long chain non-aromatic carotenoids.[2] Thus, the aromatic end groups do not imply any large modification of the excited-state level structure as compared to carotenoids substituted with ionone rings and open chain terminal groups. There are some indications in the kinetics (for example the negative amplitude kinetic feature of 110 fs which extends far into the red regions at 700 nm) which point towards higher complexity

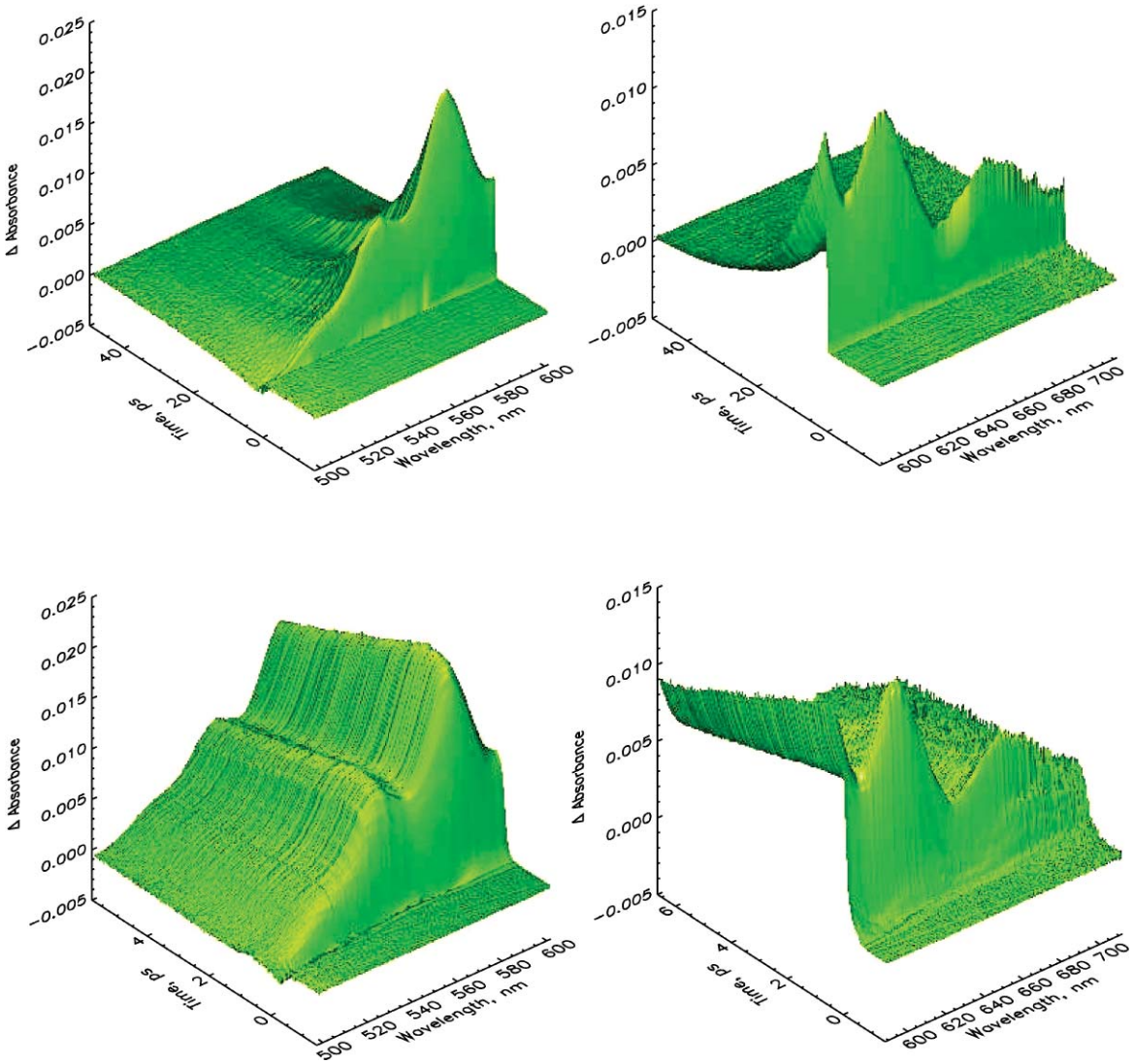

Fig. 5 Kinetics maps (Δ absorbance *vs.* wavelength *vs.* time delay) of the femtosecond transient absorption of DHIR in ethanol excited at 493 nm. The data are shown for two detection ranges (left and right figures) and two time resolutions (upper and lower figures).

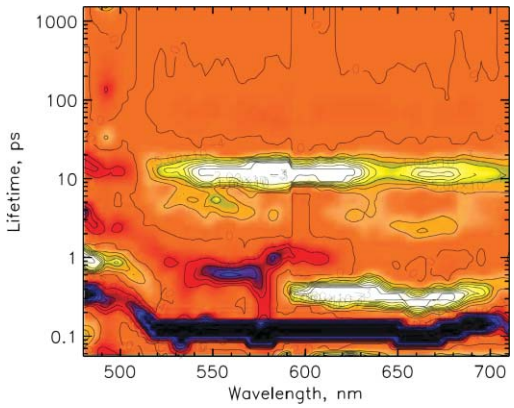

Fig. 6 Lifetime map of the femtosecond transient absorption of DHIR in ethanol excited at 493 nm. White-yellow regions correspond to positive amplitudes and reflect either absorption decay or rise of a bleaching. Blue-black regions correspond to negative amplitudes and reflect either absorption rise or decay of the bleaching.

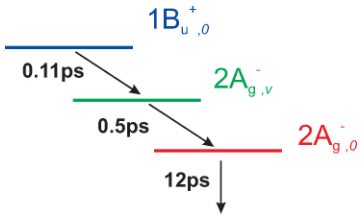

Fig. 7 Decay scheme with lifetimes of the excited states of DHIR from femtosecond transient absorption.

of the kinetics than described by the scheme in Fig. 7. The most likely reason might be the necessity to involve the $^1B_u^-$ state into the kinetic description to some extent.

Conclusions

In this work the effect of *para*-phenol and quinoid end groups on the spectral properties of carotenoids was investigated by means of experimental and quantum chemical methods. In both of the phenolic carotenoids DHIR and DHHC, aromatic end groups participate only partially in the conjugation system because they are twisted out of the molecular plane. As shown for DHIR, methyl groups in *ortho* position of the phenyl ring increase the steric repulsion between the ring and the polyene chain. Thus, its spectral properties closely resemble those of β-carotene. Early events after femtosecond absorption indicate that in addition to the $2^1A_g^-$ (S_1) state another electronic state, presumably the close-by $1^1B_u^-$ state, might play a role in the decay kinetics of the optically bright $1^1B_u^+$ state. In contrast to phenolic groups, the quinoid end groups of DHIRQ are fully integrated into the conjugation system. The increased conjugation length combined with two exocyclic double bonds does not only lead to a marked spectral shift of the visible absorption, noticeable in the blue color of the solution. It also favors doubly excited electronic configurations which are important contributors to the $2^1A_g^-$ and $1^1B_u^-$ states. Furthermore, low-lying internal charge-transfer states are found in the quantum chemical calculations. They result from single excitations of a C=O in-plane n electron to the delocalized π-electron system. Further investigations will have to show whether the increased energy gap between the $2^1A_g^-$ and the optically bright $1^1B_u^+$ states of DHIRQ has consequences on the relaxation dynamics of this compound and which role the intermediate dark states, predicted by the quantum chemical calculations, will play.

Acknowledgements

The present work has been performed as a project of the SFB 663 (B1, B2, C1) at the Heinrich-Heine-University Düsseldorf and is printed at its instigation with financial support provided by the Deutsche Forschungsgemeinschaft.

References

1 W. Kohl, H. Achenbach and H. Reichenbach, *Phytochemistry*, 1983, **22**, 207.
2 F. P. Rattray and F. P. Fox, *J. Dairy Sci.*, 1999, **82**, 891.
3 H.-D. Martin, S. Kock, R. Scherrers, K. Lutter, T. Wagener, C. Hundsdörfer, S. Frixel, K. Schaper, H. Ernst, W. Schrader, H. Görner and W. Stahl, *Angew. Chem.*, accepted.
4 S. Kock, Dissertation, Heinrich-Heine-University Düsseldorf, 2008.
5 B. S. Hudson and B. E. Kohler, *J. Chem. Phys.*, 1973, **59**, 4984.
6 T. Polívka, J. L. Herek, D. Zigmantas, H.-E. Åkerlund and V. Sundström, *Proc. Natl. Acad. Sci. USA*, 1999, **96**, 4914.
7 P. Tavan and K. Schulten, *J. Chem. Phys.*, 1979, **70**, 5407.
8 P. O. Andersson, S. B. Bachilo, R.-L. Chen and T. Gillbro, *J. Phys. Chem.*, 1995, **99**, 16199.
9 T. Sashima, Y. Koyama, T. Yamada and H. Hashimoto, *J. Phys. Chem. B*, 2000, **104**, 5011.
10 G. Cerullo, D. Polli, G. Lanzani, S. De Silvestri, H. Hashimoto and R. J. Codgell, *Science*, 2002, **298**, 2395.
11 F. S. Rondonuwu, Y. Watanabe, R. Fujii and Y. Koyama, *Chem. Phys. Lett.*, 2003, **376**, 292.
12 M. Yoshizawa, H. Aoki, M. Ue and H. Hashimoto, *Phys. Rev. B*, 2003, **67**, 174302.
13 D. S. Larsen, E. Papagiannakis, I. H. M. van Stokkum, M. Vengris, J. T. M. Kennis and R. van Grondelle, *Chem. Phys. Lett.*, 2003, **381**, 733.
14 H. Hashimoto, K. Yanagi, M. Yoshizawa, D. Polli, G. Cerullo, G. Lanzani, S. De Silvestri, A. T. Gardiner and R. J. Cogdell, *Arch. Biochem. Biophys.*, 2004, **430**, 61.
15 D. Polli, G. Cerullo, G. Lanzani, S. De Silvestri, K. Yanagi, H. Hashimoto and R. J. Cogdell, *Phys. Rev. Lett.*, 2004, **93**, 163002.
16 F. S. Rondonuwu, K. Yokoyama, R. Fujii, Y. Koyama, R. J. Cogdell and Y. Watanabe, *Chem. Phys. Lett.*, 2004, **390**, 314.
17 W. Wohlleben, T. Buckup, H. Hashimoto, R. J. Cogdell, J. L. Herek and M. Motzkus, *J. Phys. Chem. B*, 2004, **108**, 3320.
18 D. Kosumi, M. Komukai, H. Hashimoto and M. Yoshizawa, *Phys. Rev. Lett.*, 2005, **95**, 213601.
19 C. M. Marian and N. Gilka, *J. Chem. Theo. Comp.*, 2008, **4**, 1501.
20 M. Kleinschmidt, C. M. Marian, M. Waletzke and S. Grimme, *J. Chem. Phys.*, accepted.
21 D. Kosumi, K. Yanagi, R. Fujii, H. Hashimoto and M. Yoshizawa, *Chem. Phys. Lett.*, 2006, **425**, 66.
22 T. Polívka and V. Sundström, *Chem. Rev.*, 2004, **104**, 2021.
23 H. M. Vaswani, C. P. Hsu, M. Head-Gordon and G. R. Fleming, *J. Phys. Chem. B*, 2003, **107**, 7940.
24 D. Zigmantas, R. G. Hiller, V. Sundström and T. Polívka, *Proc. Natl. Acad. Sci. USA*, 2002, **99**, 16760.
25 R. Pariser, *J. Chem. Phys.*, 1956, **24**, 250.
26 B. E. Kohler and T. Itoh, *J. Phys. Chem.*, 1988, **92**, 5120.
27 R. Croce, M. G. Müller, R. Bassi and A. R. Holzwarth, *Biophys. J.*, 2001, **80**, 901.
28 A. Schaefer, H. Horn and R. Ahlrichs, *J. Chem. Phys.*, 1992, **97**, 2571.
29 W. Kohn and L. Sham, *J. Phys. Rev. A*, 1965, **140**, 1133.
30 A. D. Becke, *J. Chem. Phys.*, 1993, **98**, 5684.
31 C. Lee, W. Yang and R. G. Parr, *Phys. Rev. B*, 1988, **37**, 785.
32 F. Furche and R. Ahlrichs, *J. Chem. Phys.*, 2002, **117**, 7433.
33 R. Ahlrichs, M. Bär, M. Häser, H. Horn and C. Kölmel, *Chem. Phys. Lett.*, 1989, **162**, 165; see also http://www.cosmologic.de.
34 S. Grimme and M. Waletzke, *J. Chem. Phys.*, 1999, **111**, 5645.
35 A. D. Becke, *J. Chem. Phys.*, 1993, **98**, 1372.

36 K. Furuichi, T. Sashima and Y. Koyama, *Chem. Phys. Lett.*, 2002, **356**, 547.
37 M. Schreiber, M. R. Silva-Junior, S. P. A. Sauer and W. Thiel, *J. Chem. Phys.*, 2008, **128**, 134110; M. R. Silva-Junior, M. Schreiber, S. P. A. Sauer and W. Thiel, *J. Chem. Phys.*, 2008, **129**, 104103.
38 C. Lambert and R. W. Redmond, *Chem. Phys. Lett.*, 1994, **228**, 495.
39 G. Marston, T. G. Truscott and R. P. Wayne, *J. Chem. Soc. Faraday Trans.*, 1995, **91**, 4059.
40 L. Herzberg and G. Herzberg, *Astrophys. J.*, 1947, **105**, 353.
41 J. F. Noxon and A. V. Jones, *Nature*, 1962, **196**, 157.
42 R. L. Gattinger, *Can. J. Phys.*, 1968, **46**, 1613.
43 P. O. Andersson, S. M. Bachilo, R.-L. Chen and T. Gillbro, *J. Phys. Chem.*, 1995, **99**, 16199.

